Journal of Thermal Science Vol.26, No.3 (2017) 235−244

DOI: 10.1007/s11630-017-0935-6 **Article ID: 1003-2169(2017)03-0235-10**

Numerical Study of Hydrogen Peroxide Thermal Decomposition in a Shock Tube

Muhammad Rizwan Bhatti[1], Nadeem Ahmed Sheikh[1*], Shehryar Manzoor[2], Muhammad Mahabat Khan[1], Muzaffar Ali[2]

1 Department of Mechanical Engineering, Capital University of Science and Technology, Islamabad, Pakistan
2 Mechanical Engineering Department, University of Engineering and Technology, Taxila, Pakistan

Hydrogen peroxide (H_2O_2) has its significance during the combustion of heavy hydrocarbons in the internal combustion (IC) engines. Owing to its importance the measurements of H_2O_2 dissociation rate have been reported mostly using the shock tube apparatus. These types of experimental measurements are although quite reliable but require high cost. On the other hand, numerical simulations provide low cost and reliable solutions especially using computation fluid dynamics (CFD) software. In the current study an experimental shock tube flow is modeled using open access platform OpenFOAM to investigate the thermal decomposition of H_2O_2. Using two different convective schemes, limitedLinear and upwind, the propagation of shock wave and resultant dissociation reaction are simulated. The results of the simulations are compared with the experimental data. It is observed that the rate constant measured using the simulation data deviates from the experimental results in the low temperature range and approaches the experimental values as the temperature is raised.

Keywords: Reaction kinetics, Rate constant, Numerical simulation, Shock wave, Reflected shock wave, Contact discontinuity, Expansion fan, Internal flow, Compressible flow, Gas dynamics

Introduction

During the combustion of fossil fuels in the internal combustion engines, numerous intermediate reactions occur before the production of final products (Bhaskaran et al. 2002). Hydrogen peroxide is one of the most important intermediate compounds formed which guides and controls the downstream chain of reactions in the temperature range of 850 K to 1200 K (Hong et al. 2011). Hydrogen peroxide is also used as monopropellant using the catalytic decomposition technique in some types of rocket engines. It has its future as a green monopropellant (Westbrook 2000). For the delivery of micro satellites in the orbits, it is an established monopropellant fuel (Davenas et al. 2004). It is also being utilized as an oxidizer in some rocket engines. It has also found its utility for the alignment of satellites and attitude control purposes. Besides hydrogen peroxide has numerous industrial applications; for instance treatment of waste water, industrial waste treatment, bleaching of textile products and bleaching of paper etc.

Due to its versatile applications, H_2O_2 dissociate reaction is extensively used experimentally. Most experimental setups used shock tube. In the shock tube environment, the propagating shock wave upon reflection from end wall provides appropriate environment (in terms of temperature and pressure) where the thermal decomposition can occur (Anderson 2003). This process has been studied using various diagnostic techniques. Bilwakesh et al. (1968) performed the thermal decompo-

Received: June 2016 N.A. Sheikh: Dr. Associate Professor

Nomenclature

A	speed of sound (m/s)	R	gas constant (joules/kg·K)
C_p	sp. heat at const. pressure (joules/kg·K)	R_l	rate of production of lth species
D_l	diffusion coefficient of lth species	s	seconds
e	specific internal energy (joules/kg)	**U**	velocity vector (m/s)
h	specific enthalpy (joules/kg)	v	velocity of contact discontinuity (m/s)
I	Identity Matrix	w	specific volume (m^3/kg)
J_l	diffusion flux of lth species	W	velocity of normal shock wave (m/s)
k	rate constant($cm^3mol^{-1}s^{-1}$)	W_r	velocity of reflected shock wave (m/s)
K	Kelvin (temperature)	Y_l	mass fraction of lth species
K	Kinetic Energy (joules)	γ	specific heat ratio
L	length (m)	∇	del operator
m	meter	ρ	density (kg/m^3)
p	Pressure in Pascal	τ	viscous tensor
Pa	Pascal (pressure)	μ	micro
q	heat flux ($Watt/m^2$)	θ	dynamic viscosity ($N{\cdot}s/m^2$)

sition analysis with the help of experimental shock tube facility. In order to monitor the thermal decomposition they utilized the absorption methods. The driver section consisted of air and helium mixture whereas the driven section consisted of H_2O_2 and nitrogen mixture. The nitrogen served as the bath gas. Meyer et al. (1969) analyzed the decomposition of N_2H_4 and H_2O_2. They measured the decomposition rate of H_2O_2 between temperatures 950 K to 1450 K and the pressure was kept up to 20 bar. UV absorption was used to monitor the decomposition rates.

Few other studies such as Trainor et al. (1974) conducted the study of reunification of OH ion using the photolysis technique at low pressure and temperature and utilized the absorption spectroscopy. Using flash photolysis Zellner et al. (1988) conducted experiments at low temperature and pressure range. Forster et al. (1995) with the help of laser induced fluorescence monitored the ions at room temperature and pressure up to 150 bar. Fulle et al. (1996) also used the laser induced fluorescence for the reunification of OH radicals. The maximum pressure and temperature were 150 bar and 700 K respectively. Sangwan et al. (2012) performed the experimental study of hydroxyl to hydroxyl reaction with the help of UV absorption monitoring technique at temperatures ranging from 296 K to 834 K and pressures ranging from 1 bar to 100 bar. Bahrini et al. (2012) performed the quantitative analysis of hydrogen peroxide. Brouwer et al. (1987) performed the theoretical calculations of reaction rates by using statistical adiabatic models. The temperature was in the range 200 K to 1500 K. Troe et al. (2008) used the ab-initio technique for the calculation of decomposition/recombination of H_2O_2 up to maximum temperature of 5000 K. This ab-initio technique is a quantum chemistry method and is a subject of computational chemistry (Levine 1991). Sellevag et al. (2009) used two transition state model for the calculation of rate constants with temperature ranging between 200 K and 3000 K.

Using shock tubes, Hong et al. (2009) conducted experiments regarding the H_2O_2 thermal decomposition. They used tunable laser absorption near 2.5×10^{-6} m to detect the H_2O in the products. Hong et al. (2010) used IR absorption for the detection of H_2O at 2.55×10^{-6} m in the temperature between 1000 K to 1200 K and pressure between 0.9 atm. to 3.2 atm. In another study, Hong et al. (2011) used UV absorption to monitor OH near 306.7×10^{-9} m and used infrared absorption to monitor water near 2.55×10^{-6} m. They measured the rate constant for hydrogen peroxide thermal decomposition at temperatures between 1020 to 1460 K and pressure at 1.8 atm. More recently, Sajid et al. (2013) performed the experiments for the analysis of thermal decomposition of H_2O_2 in a shock tube and used quantum cascade laser absorption near 7.7×10^{-6} m. They performed the experiments in temperature range 930 – 1235 K and for pressures at 1, 2 and 10 atm.

As briefed above, most of the work in this area is experimental. On the other hand, Computational Fluid Dynamics (CFD) is a fast growing area to simulate the expensive physical experiments. Due to cheap availability of computers and state of the art softwares/tools which are both open source and freely available, it has become feasible to perform simulations in a rapid and cost effective manner. To harness the potential of CFD, the experimental setup described by Sajid et al. (2013) has been simulated in an open source OpenFOAM software. One of its solvers, reactingFoam has been used to perform the simulations using the limitedLinear and upwind convec-

tive schemes. The reactingFoam solver supports the reaction kinetics. The thermal decomposition analysis of hydrogen peroxide has been conducted by modeling the experimental shock tube and the results have been compared with the experimental results.

Shock Tube analytical model

Theory

The shock tube is a circular or rectangular pipe with both ends closed. The shock tube for the current study has circular cross-section. A thin membrane called diaphragm divides the shock tube into two compartments. In Fig. 1 the left compartment is called the driver section and is denoted by '4'. The right compartment is called the driven section and is denoted by '1'. Both compartments are filled with gas whereas the pressure of driver section is greater than the driven section. Both the sections can have the same gas or different gases. Similarly both compartments may have the same temperature or different temperature.

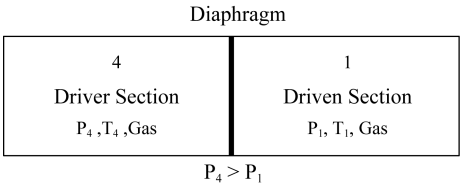

Fig. 1 Initial Profile of Shock Tube

The velocities in both compartments are initially zero. Suppose that P_1, T_1 are pressure and temperature in compartment 1 and P_4, T_4 are pressure and temperature in compartment 4. Then the pressure ratio P_4/P_1 is said to be the diaphragm pressure ratio.

Figure 2 shows different regions formed due to sudden removal of diaphragm by some mechanism. The region 1 and 2 is separated by normal shock wave which is heading towards right. The region 2 and 3 are separated by contact discontinuity. There is an expansion fan in between the regions 3 and 4. The regions 2 and 3 have same velocity and pressure but different temperature and density.

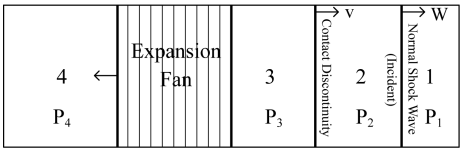

Fig. 2 Pre Shock Reflection Scenario

Figure 3 is depicting the post shock reflection scene. When the shock is reflected back after striking the end wall of driven compartment, the region 5 appears. It has comparatively high pressure and temperature and zero velocity.

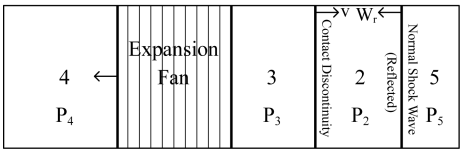

Fig. 3 Post Shock Reflection Scenario

Governing Equations

The movement of shock wave in the shock tube can be modeled analytically using continuity, momentum and energy balance across the normal shock wave.

$$\rho_1 W = \rho_2 (W - v) \tag{1}$$

$$p_1 + \rho_1 W^2 = p_2 + \rho_2 (W - v)^2 \tag{2}$$

$$e_1 + \frac{p_1}{\rho_1} + \frac{W^2}{2} = e_2 + \frac{p_2}{\rho_2} + \frac{(W - v)^2}{2} \tag{3}$$

Here ρ denotes density, W represents shock velocity, v is the velocity of contact discontinuity, p represents pressure and e Here ρ denotes density, W represents shock velocity, v is the velocity of contact discontinuity, p represents pressure and e is the internal energy. The Eq. (4) is the Hugoniot equation, whereas w represents the specific volume.

$$e_2 - e_1 = \left(\frac{p_2 + p_1}{2}\right)(w_1 - w_2) \tag{4}$$

The Eq. (5) provides the shock strength $\frac{p_2}{p_1}$ from which the unknown value of p_2 is obtained.

$$\frac{p_2}{p_1}\left[1 - \frac{(\gamma_4 - 1)(a_1/a_4)(p_2/p_1 - 1)}{\sqrt{2\gamma_1\left(2\gamma_1 + (\gamma_1 + 1)\right)(p_2/p_1 - 1)}}\right]^{-2\gamma_4/(\gamma_4 - 1)} = \frac{p_4}{p_1} \tag{5}$$

Where γ is the specific heat ratio and a represents the speed of sound.

The Eqs. (6) – (8) represent the mass, momentum and energy equations respectively for the reflected shock.

$$\rho_2 (W_r + v) = \rho_5 W_r \tag{6}$$

$$p_2 + \rho_2 (W_r + v)^2 = p_5 + \rho_5 W_r^2 \tag{7}$$

$$h_2 + \frac{(W_r + v)^2}{2} = h_5 + \frac{W_r^2}{2} \tag{8}$$

Where W_r is the velocity of the reflected shock and h is the enthalpy.

Numerical modeling

The Navier Stokes equations along with the species transport equation are given by

$$\frac{\partial \rho}{\partial t} + \nabla \cdot (\rho \mathbf{U}) = 0 \tag{9}$$

$$\frac{\partial (\rho \mathbf{U})}{\partial t} + \nabla \cdot (\rho \mathbf{U}\mathbf{U}) = \nabla \cdot \mathrm{p} + \nabla \cdot \tau \tag{10}$$

$$\frac{\partial (\rho h)}{\partial t} + \nabla \cdot (\rho h \mathbf{U}) + \frac{\partial (pK)}{\partial t} + \nabla \cdot (\rho K \mathbf{U}) - \frac{dp}{dt} = -\nabla \cdot \mathbf{q} + \nabla \cdot (\tau \cdot \mathbf{U}) \tag{11}$$

$$\frac{\partial(\rho Y_l)}{\partial t}+\nabla\cdot(\rho Y_l \mathbf{U})+\nabla\cdot\boldsymbol{J_l}=R_l \quad (12)$$

$$\boldsymbol{J_l}=-\rho D_l \nabla \boldsymbol{Y_l} \quad (13)$$

$$\tau=\vartheta\left[\nabla\boldsymbol{U}+(\nabla\boldsymbol{U})^{\boldsymbol{T}}\right]+\frac{2}{3}\vartheta(\nabla\cdot\boldsymbol{U})\boldsymbol{I} \quad (14)$$

$$p = \rho RT \quad (15)$$

Where **U** is velocity vector, τ represents viscous tensor, ***I*** is the identity matrix, θ is dynamic viscosity, K represents kinetic energy, $\boldsymbol{Y_l}$ is mass fraction of l^{th} species, $\boldsymbol{J_l}$ is the diffusion flux *of* l^{th} species, R_l represents production rate of the l^{th} species, D_l is diffusion coefficient, R is the gas constant, **q** is heat flux, ρ is density, p is the pressure, and h is the enthalpy. The chemical reaction and the rate constant for the reaction are given by Eq. (19) and Eq. (20) respectively.

Solver

The OpenFOAM supports a diverse range of solvers including the pressure based and density based solvers. The shock tube phenomena can be modeled by sonicFoam pressure based solver and rhoCentralFoam density based solver. But these solvers work in inert scenario only. As has been previously mentioned that reactingFoam solver in OpenFOAM supports reaction kinetics. However it is a pressure based generic solver in which intermediate or global reactions can be modeled. Therefore, it has been chosen as a suitable candidate to simulate the thermal decomposition of hydrogen peroxide by modeling the shock tube apparatus.

The reactingFoam solver consists of PIMPLE algorithm. It is a combination of SIMPLE and PISO algorithms. The k-epsilon turbulence model has been used for the current study due to its robustness and accuracy. It is also suitable for confined flows (Versteeg 2007). In order to compute the dynamic viscosity, the Sutherland transport model has been used. C_p is calculated using the JANAF tables for the species (McBride 1993). The Partially Stirred Reactor (PaSR) combustion model has been used to model the combustion phenomena (Correa 1993). It is a modification of Eddy Dissipation Concept (EDC). The species considered in the simulations are H_2O_2, H_2O, OH, Ar and He.

For the time discretization, the Euler implicit scheme has been utilized which is first order and bounded. In order to interpolate the diffusion coefficient, the linear interpolation scheme has been utilized. To discretize the surface normal gradient the uncorrected scheme has been implemented which is first order and bounded.

Convective Schemes

For the aforementioned case two different convective schemes, LimitedLinear and upwind, are used. LimitedLinear falls into the helm of Total Variation Diminishing (TVD) schemes (Direct 2015). It is bounded and is of second order.

Figure 4 represents the control volume around P. E and W are east and west nodes. e is the cell interface. The fluxes are calculated at cell interfaces.

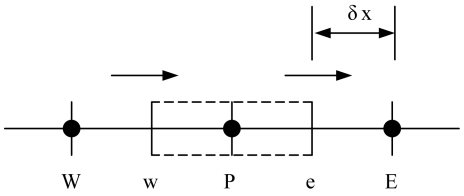

Fig. 4 Control Volume around P

Using Fig. 4, the central difference scheme is given by

$$\phi_e=\phi_P+\frac{1}{2}\varphi(r)(\phi_E-\phi_P) \quad (16)$$

Where ϕ_e is flux at the cell interface e, $\varphi(r)$ is flux limiter and for the case of central difference $\varphi(r)=1$. The limitedLinear scheme is obtained by replacing the flux limiter of central difference scheme with the Sweby flux limiter. The Sweby limiter is given by Eq. (17) (Versteeg 2007)

$$\varphi(r)=\max\left[0,\min(1.5r,1),\min(r,1.5)\right] \quad (17)$$

The upwind scheme is first order bounded. It is given by Eq. (18)

$$\phi_e = \phi_P \quad (18)$$

Behavior of Convective Schemes

In order to compare the results of convective schemes with the analytical results, each simulation for limitedLinear and upwind schemes has been run by using the reactingFoam solver. Initially laminar and inert settings have been taken for the simulations. Air has been taken as the working inert gas. The simulation is 1-D and the mesh resolution is 200 computational cells.

Table 1 Shock Tube Specs

Quantity	Symbol	Value
Driver Length	L_1	0.1 m
Driven Length	L_2	0.1 m
Total Length	$L_1 + L_2$	0.2 m
Driver Pressure	P_4	1000,000 pa.
Driver Temperature	T_4	800 K
Driven Pressure	P_1	100,000 pa.
Driven Temperature	T_1	300 K

Figures 5 and 6 show almost the same results in both cases of limitedLinear and upwind schemes. There is only slight difference in the overshoot at the normal shock. The overshoot is more prominent in case of limi-

tedLinear. The normal shock wave in analytical case is lagging behind the numerical shock predictions.

Both schemes have shown that the pressure and velocity are the same in regions 2 and 3 which conform to the physics of the problem. There is an over prediction in pressure and an under prediction in velocity in both cases. The contact discontinuity has been captured in both cases, which has been shown in the temperature and density

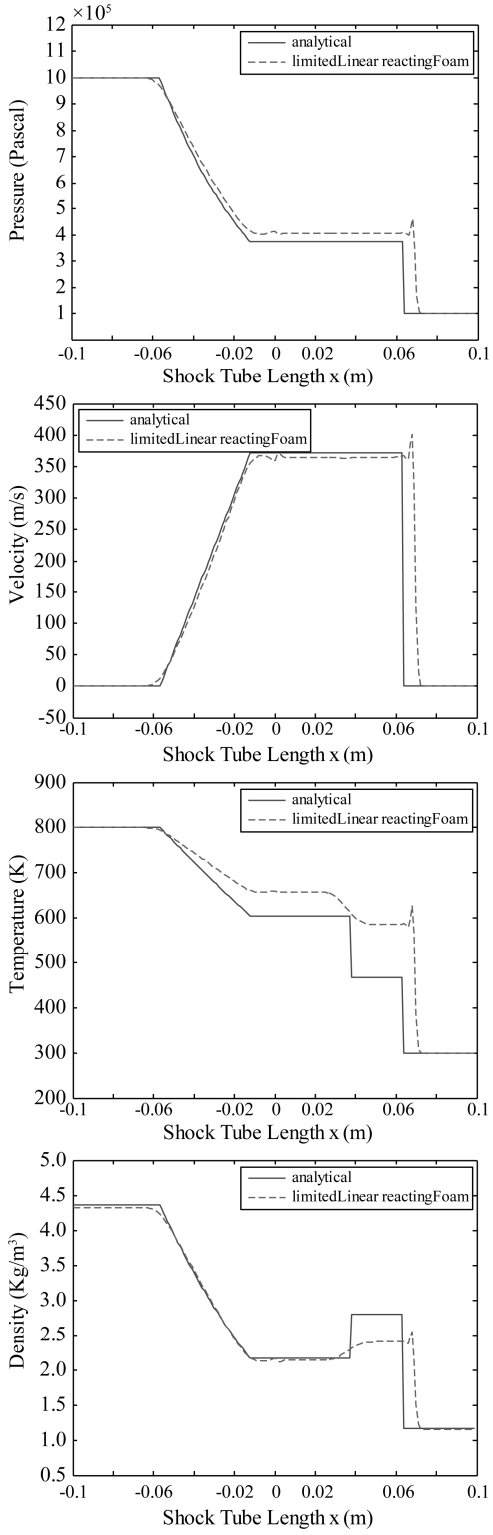

Fig. 5 limitedLinear and analytical results

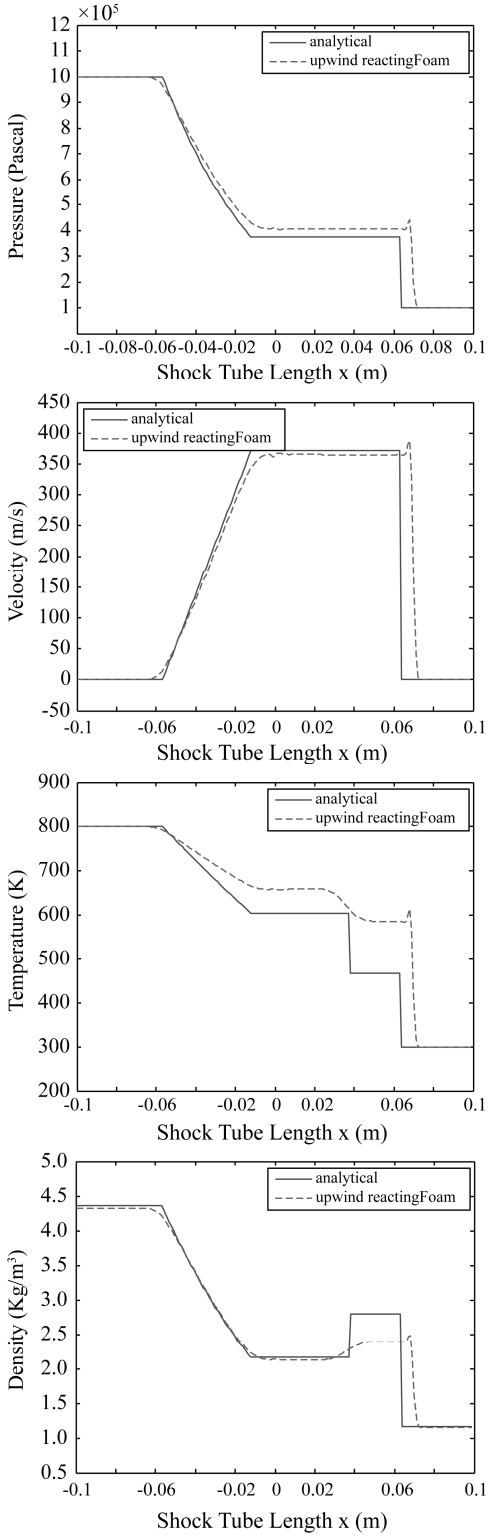

Fig. 6 Upwind and analytical results

plots. The temperature is over predicted in both regions but the difference is less in region 3 as compared to region 2. The results are very good in case of density in region 3 and there is under prediction in the case of region 2.

Comparison of reactingfoam results with experimental data

This section provides the details of the results of reactingFoam simulations regarding the thermal decomposition of hydrogen peroxide in the shock tube model. The reactingFoam solver has been run for both limitedLinear and upwind convective schemes.

Summary of Experimental Data

Sajid Es-Sebbar et al. (2013) experimental data has been taken to run the reactingFoam simulations. Sajid used analytical model to calculate temperature and pressure in region 5. Equation (19) represents the hydrogen peroxide decomposition reaction while Eq. (20) is its rate constant measured from the experiment. It has been entered as an input to the reactingFoam solver.

$$H_2O_2 + Ar \rightarrow 2OH + Ar \tag{19}$$

$$k(T)_{at\ 1,2\ atms} = 10^{(16.29\pm0.12)} \times \exp(-21993 \pm 301/T) \quad \left(cm^3 mol^{-1} s^{-1}\right) \tag{20}$$

Simulation Results (limitedLinear)

1-D shock tube simulations have been run using 4000, 6000 and 8000 spatial resolutions using limitedLinear as the convective scheme. The purpose to use different mesh resolutions is to ensure the mesh resolution independence for thermal decom-position of hydrogen peroxide. Each simulation has been run for time duration of 16 milliseconds with the initial time step of 5×10^{-7} seconds. The shock tube specifications used are detailed in Table 2. The driver section comprised of helium gas. The driven section consists of gas mixture as mentioned in Table 3.

Table 2 Shock Tube Specs

Quantity	Symbol	Value
Driver Length	L_1	4.5 m
Driven Length	L_2	9 m
Total Length	$L_1 + L_2$	13.5 m
Driver Pressure	P_4	107998 Pa
Driver Temperature	T_4	800 K
Driven Pressure	P_1	12000 Pa
Driven Temperature	T_1	296 K

Table 3 Mole Fraction of Gases (Driven Section)

Gas	Mole Fractions
Argon	0.991
H_2O_2	0.005
H_2O	0.004

A probe has been placed at 13.495 m from the origin, so that the thermal decomposition data, temperature, pressure and velocity could be recorded. The probe location has been finalized to ensure the maximum temperature of post reflection region, since the temperature falls drastically as the reflected normal shock gets away from the driven section end wall. This phenomenon of reflected shock wave can be viewed in Fig. 7.

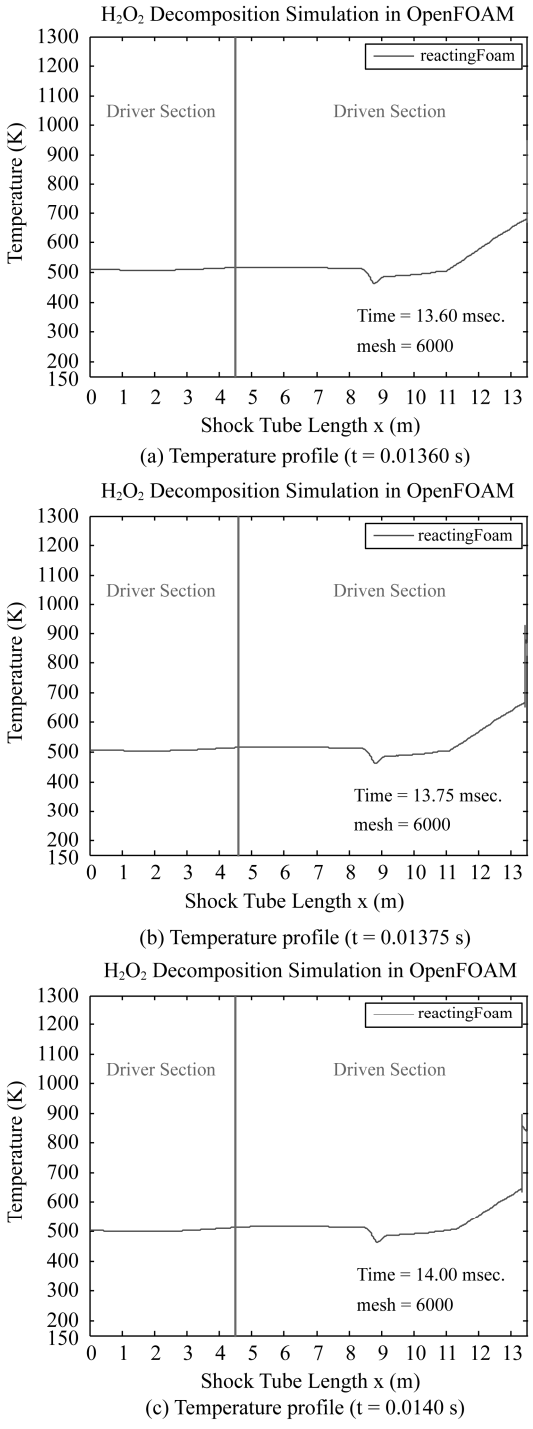

(a) Temperature profile (t = 0.01360 s)

(b) Temperature profile (t = 0.01375 s)

(c) Temperature profile (t = 0.0140 s)

Fig. 7

The thermal decomposition profile for 250 μs from the beginning of decomposition in the post reflection region 5 at the specified probe for the mesh resolution 6000 is shown in Fig. 8.

The velocity, temperature and pressure scenarios for the 250 μs thermal decomposition duration have been shown by Figs. 9, 10 and 11 respectively.

It has been observed that the temperature plot could not capture the contact discontinuity. The region 2 temperature is nearly 690 K, which agrees well with the temperature 696.94 K predicted by WGD calculator for this region. The pressure for the region 2 is 58000 Pa, which is comparable to 69643 Pa predicted by WGD calculator for this region. The pressure and temperature values predicted by the reactingFoam solver, with limitedLinear convective scheme, in region 5 were lower as compared to WGD calculator values and the experimental values (see Table 4). The pressure and temperature values in region 5 as reported by Sajid et al. are also based on the analytical equations. The comparison of hydrogen peroxide mole fraction profile with the experimental data has been analyzed in section 4.4. It also has been observed that the thermal decomposition profiles are not changing significantly by changing mesh resolution from 4000 to 8000. So it is safe to consider the mesh independence of hydrogen peroxide decomposition profile at 6000 mesh resolution.

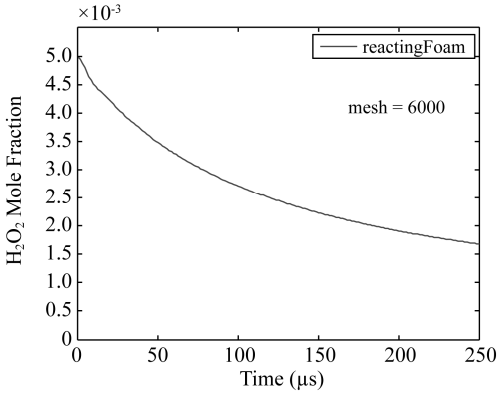

Fig. 8 H_2O_2 mole fraction time history

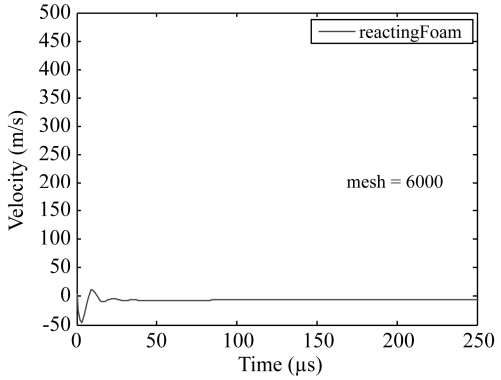

Fig. 9 Velocity profile during thermal decomposition of H_2O_2

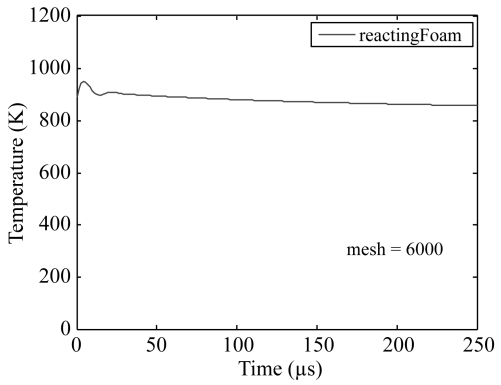

Fig. 10 Temperature profile during thermal decomposition of H_2O_2

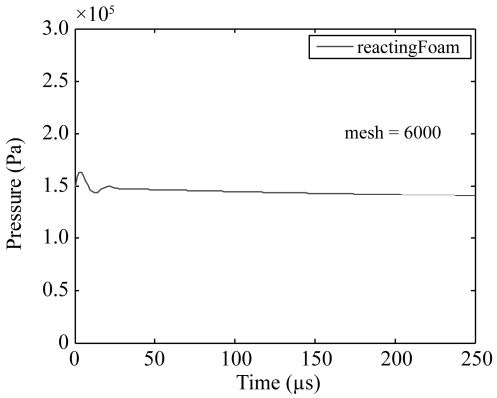

Fig. 11 Pressure profile during thermal decomposition of H_2O_2

Table 4 Temperatures and Pressures (Region 5)

Source	Temperature T_5 (K)	Pressure P_5 (atmospheres)
(Sajid et al. 2013)	1167	2.35
(WGD 2008)	1211.45	2.3687
limitedLinear 4000 mesh	875.4	1.45
limitedLinear 6000 mesh	878.59	1.42
limitedLinear 8000 mesh	874.62	1.415

Simulation Results (upwind)

Table 5 shows the temperature and pressure values in region 5 produced by reactingFoam upwind case at mesh resolution 6000.

It is observed that the velocity remains the same in region 2 as has been predicted by limitedLinear based simulation. It has been observed that like the limitedLinear scheme, the upwind scheme also could not capture the contact discontinuity. The temperature in region 2 is almost 700 K. The pressure in region 2 is 60000 Pa. Figure 14 shows that the temperature for upwind case has in-

creased as compared to limitedLinear. It has resulted in more dropping of the mole fractions of hydrogen peroxide in case of upwind as shown in Fig. 12.

Table 5 Temperatures and Pressures (Region 5)

Source	Temperature T_5 (K)	Pressure P_5 (atmospheres)
(Sajid et al. 2013)	1167	2.35
(WGD 2008)	1211.45	2.3687
upwind 6000 mesh	911.61	1.496

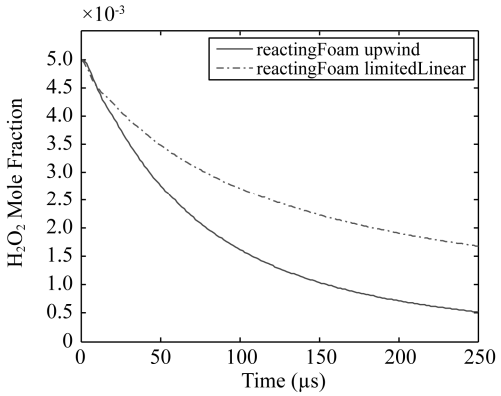

Fig. 12 H_2O_2 mole fraction time history (at probe location)

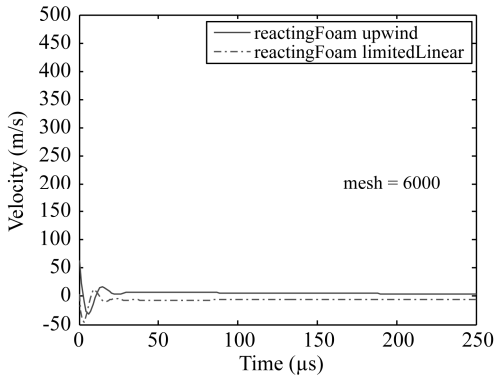

Fig. 13 Velocity profile during thermal decomposition of H_2O_2

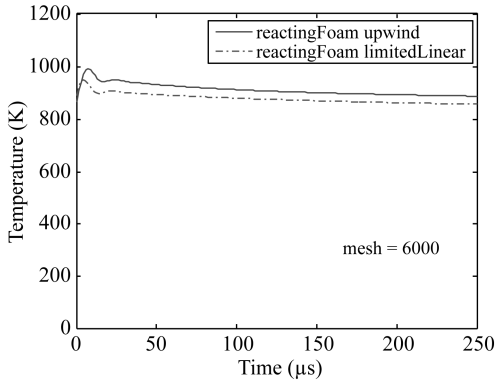

Fig. 14 Temperature profile during thermal decomposition of H_2O_2

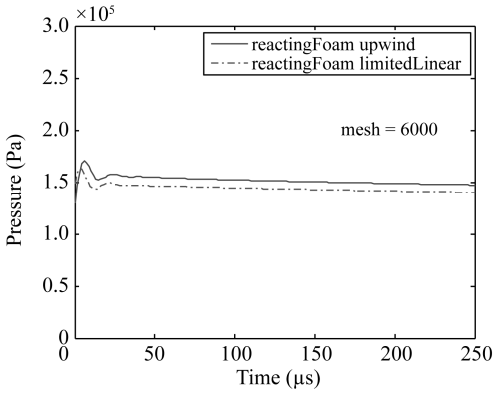

Fig. 15 Pressure profile during thermal decomposition of H_2O_2

Comparison of Results

Figure 16 is the comparison of the hydrogen peroxide thermal decomposition profiles of the limitedLinear and upwind schemes with the Sajid et al. experimental results.

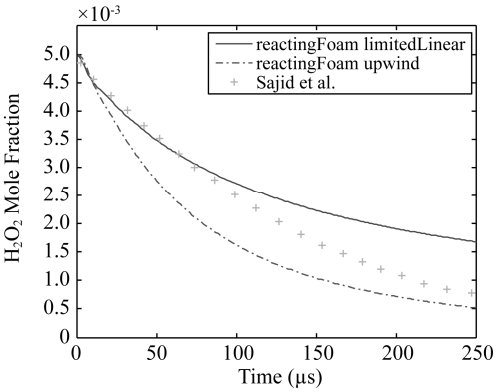

Fig. 16 H_2O_2 Decomposition Profile (at probe location)

The Sajid et al. data is shown by '+' sign, which serves as the reference. The results shown by limitedLinear and upwind schemes are for the 6000 grid resolution. The plots for limitedLinear and upwind cases are for average temperatures 878.59 K and 911.61 K respectively. The average pressure values in region 5 for these two schemes are 1.42 atm. and 1.469 atm. respectively. Sajid et al. reported the temperature 1167 K and pressure 2.35 atm. for this region, which are based on analytical computations.

Sajid et al. plot represents the exponential decay in the mole fraction of hydrogen peroxide, which is a non-linear phenomenon. Figure 16 shows that the limitedLinear and upwind cases also follow the same type of non-linear behavior. The limitedLinear curve overlaps the Sajid et al. curve from the start of decomposition point up to 100 s. Afterwards it deviates due to reduction in decay rate and finally it terminates the graph at

250 s to the value of 0.00168, which is higher than the experimental mole fraction value 0.00078 at this point.

The upwind curve shows fast exponential decay in the mole fraction as compared to experimental data during the first half section. The second half portion of the curve shows the comparatively low decomposition rate. The curve finally ends the graph with slightly lower value than the experimental value of mole fraction. The fast exponential decay of mole fraction is attributed to the high temperature obtained in the upwind scheme as compared to the limitedLinear scheme. The latter parts of the curves in both cases show decrease in the decomposition rates, which is due to sharp decrease in temperature. It is again mentioned here that Sajid et al. used the values of temperature and pressure on the basis of analytical equations.

Table 6 shows the relation between rate constant k and 1000/T, where T represents temperature. The results of Sajid et al. and Hong et al. are for pressure 2 atmospheres and 1.7 atmospheres respectively, which have been shown for comparison. The limitedLinear results have also been shown. The limitedLinear results deviate from the Sajid et al. and Hong et al. results at lower temperatures and approach the experimental values as the temperature is increased.

Table 6 Rate constant vs Temperature

Source	1000/T (1/K)	k ($cm^3 \cdot mol^{-1} \cdot s^{-1}$)
limitedLinear	1.1382	1.44×10^8
	1.0763	1.95×10^8
	0.9730	4.42×10^8
	0.8857	2.95×10^8
Sajid et al. (2013)	1.0639	1.44×10^6
	1.0029	5.16×10^6
	0.9475	1.61×10^7
	0.9057	4.54×10^7
	0.8568	1.44×10^8
	0.8319	2.47×10^8
Hong et al. (2011)	0.9924	8.50×10^6
	0.9812	9.77×10^6
	0.9724	1.15×10^7
	0.9563	1.61×10^7
	0.9378	2.40×10^7
	0.8953	5.65×10^7
	0.8913	6.77×10^7
	0.8648	1.01×10^8
	0.8552	1.28×10^8
	0.8407	1.95×10^8
	0.8319	2.11×10^8

Conclusion

The importance of hydrogen peroxide can be gauged from the fact that it is produced in the bulk quantities as an intermediate compound during the combustion of fossil fuels in various types of engines. It controls the chain of intermediate reactions leading to the final formation of products. It is used as fuel in some kinds of rockets, whereas it is also used as oxidizer in some other types of rocket systems. It is also used in industry.

In the present study, the shock tube model of an experimental setup has been simulated using the reactingFoam solver in the OpenFOAM. The results of limitedLinear and upwind convective schemes have been discussed and compared with the experimental results. The thermal decomposition curves produced by the limitedLinear and upwind convective schemes agree well with the experimental curve as shown in Fig. 16. The rate constant k in case of limitedLinear has been computed at different temperatures. Table 6 shows that it deviates from the experimental results at low temperatures and agrees well to the experimental values as the temperature is raised.

References

[1] "WiSTL Wisconsin Shock Tube Laboratory, Gas Dynamics Calculator." Retrieved 14th June 2015, 2015, from http://silver.neep.wisc.edu/~shock/tools/gdcalc.html.

[2] Anderson, J. D. (2003). Modern Compressible Flow with Historical Perspective. New York, Mc Graw Hill.

[3] Bahrini, C., O. Herbinet, P.-A. Glaude, C. Schoemaecker, C. Fittschen and F. Battin-Leclerc (2012). "Quantification of Hydrogen Peroxide during the Low-Temperature Oxidation of Alkanes." J. Am. Chem. Soc. 134: 11944−11947.

[4] Bhaskaran, K. A. and P. Roth (2002). "The shock tube as wave reactor for kinetic studies and material systems." (28): 151−192.

[5] Bilwakesh, K. R., W. A. Strauss, R. Edse and E. S. Fishburne (1968). The Thermal Decomposition of Hydrogen Peroxide Vapor. Columbus, Ohio: 28.

[6] Bonnie J. McBride, S. G., Martin A. Reno. (1993). "Coefficients for Calculating Thermodynamic and Trasport Properties of Individual Species." Retrieved 16th August, 2015, from http://ntrs.nasa.gov/archive/nasa/ casi.ntrs.nasa.gov/19940013151.pdf.

[7] Brouwer, L., C. J. Cobos, J. Troe, H. R. Dubal and F. F. Crim (1987). "Specific rate constants k(E, J) and product state distributions in simple bond fission reactions. II. Application to HOOH - OH+OH." J. Chem. Phys. 86: 6171.

[8] Correa, S. M. (1993). "Turbulence-chemistry interactions

in the intermediate regime of premixed combustion." Combustion and Flame 93(1−2): 41−60.

[9] Davenas, A., G. Jacob, Y. Longevialle and C. Perut (7-8 June 2004). Energetic Compounds for Future Space Applications. proc. '2nd Int. Conference on Green Propellants for Space Propulsion', Cagliari, Sardinia, Italy.

[10] Direct, C. (2015). "OpenFOAM User Guide: 4.4 Numerical schemes." Retrieved 14th June, 2015, from http://cfd.direct/openfoam/user-guide/fvSchemes/.

[11] Forster, R., M. Frost, D. Fulle, H. Hamann, H. Hippler, A. Schlepegrell and J. Troe (1995). "High pressure range of the addition of HO to HO, NO, NO2, and CO. I. Saturated laser induced fluorescence measurements at 298 K." J Chem. Phys. 103.

[12] Fulle, D., H. F. Hamann, H. Hippler and J. Troe (1996). "High - pressure range of the addition of HO to HO. III. Saturated laser - induced fluorescence measurements between 200 and 700 K." J. Chem. Phys. 105

[13] Hong, Z., R. D. Cook, D. F. Davidson and R. K. Hanson (2010). "A Shock Tube Study of OH + H2O2 -> H2O+HO2 and H2O2 + M -> 2OH + M using Laser Absorption of H2O and OH." J. Phys. Chem. A 114: 5718−5727.

[14] Hong, Z., D. F. Davidson and R. K. Hanson (2011). "An improved H2/O2 mechanism based on recent shock tube/laser absorption measurements." Combustion and Flame 158: 633−644.

[15] Hong, Z., A. Farooq, E. A. Barbour, D. F. Davidson and R. K. Hanson (2009). "Hydrogen Peroxide Decomposition Rate: A Shock Tube Study Using Tunable Laser Absorption of H2O near 2.5 micro meter." J. Phys. Chem. A 113: 12919−12925.

[16] Levine, I. N. (1991). Quantum Chemistry. Englewood Cliffs, New jersey, Prentice Hall.

[17] Meyer, E., H. A. Olschewski, J. Troe and H. G. Wagner (1969). "Investigation of N2H4 and H2O2 decomposition in low and high pressure shock waves." Symposium (International) on Combustion 12(1): 345−355.

[18] Sajid, M. B., E. Es-Sebbar, T. Javed, C. Fittschen and A. Farooq (2013). "Measurement of the Rate of Hydrogen Peroxide Thermal Decomposition in a Shock Tube Using Quantum Cascade Laser Absorption Near 7.7 micro meter." International Journal of Chemical Kinetics 46(5): 275–284.

[19] Sangwan, M., E. N. Chesnokov and L. N. Krasnoperov (2012). "Reaction OH + OH Studied over the 298-834 K Temperature and 1 - 100 bar Pressure Ranges." J. Phys. Chem. A 116: 6282−6294.

[20] Sellevag, S. R., Y. Georgievskii and J. A. Milller (2009). "Kinetics of the Gas-Phase Recombination Reaction of Hydroxyl Radicals to Form Hydrogen Peroxide." J. Phys. Chem. A 113: 4457−4467.

[21] Trainor, D. W. and C. W. J. v. Rosenberg (1974). "Flash photolysis study of the gas phase recombination of hydroxyl radicals." J. Chem. Phys. 61.

[22] Troe, J. and V. G. Ushakov (2008). "SACM/CT Study of the dissociation/recombination dynamics of hydrogen peroxide on an ab initio potential energy surface Part II. Specific rate constants k(E,J), thermal rate constants k N (T), and lifetime distributions." Phys. Chem Chem Phys. 10: 3915−3924.

[23] Versteeg, H. K. and W. Malalasekera (2007). An Introduction to Computational Fluid Dynamics, The Finite Volume Method. Harlow, England, Pearson, Prentice Hall.

[24] Westbrook, C. K. (2000). "Chemical Kinetics of Hydrocarbon Ignition in Practical Combustion Systems." Proceedings of the Combustion Institute 28: 1563−1577.

[25] Zellner, R., F. Ewig, R. Paschke and G. Wagner (1988). "Pressure and Temperature Dependence of the Gas-Phase Recombination of Hydroxyl Radicals." J. Phys. Chem. 92: 4184−4190.